Development of a Flame Calorimeter

Ki Won LIM
Center for Fluid Flow & Acoustics/Korea Research Institute of Standards and Science, Daejeon, Korea
Tel:82-42-868-5314 , Fax:82-42-868-5028, E-mail:kwlim@kriss.re.kr

Jin Yong Jun*, Byeong-Jun Lee**
Dept. of Mech. Eng., Yeungnam University, Gyeongsan, Gyeongbuk, Korea
Tel:82-53-810-3526, Fax:82-53-810-4627, E-mail:bjlee@yu.ac.kr
*:Graduate School, **:Professor

Abstract: The calorific value of Natural Gas (NG), as a mixed gas fuel, strongly depends on composition. The composition of NG is mainly methane, ethane, propane, butane and nitrogen, which varies with time and place it was produced. In order to measure the calorific value of NG, a flame calorimeter was manufactured and characterized in this study. For development of the flame calorimeter, the electric substitution method initiated by Alexandrov was applied. Peltier elements on the calorimeter emit the heat supplied by a heater and a flame under the thermal equilibrium state. Freon-11 was used as a heat carrier for steady state heat flow. It was proved that the calorific value of methane as measured with the calorimeter deviates by -0.36 % from the theoretical entalpy.

Keywords: Flame calorimeter, Natural gas, Electric substitution method, Mehtane

1. Introduction

Last decade, the shortage of energy resources led to the development of new gas fields in various places around the world. The composition of the natural gas from these fields, as a mixed gas fuel, depends on where and when it was produced. Table 1 shows the variations of the NG compositions from difference sources. Calorific value depends on the composition of the natural gas. These variations of the calorific value of the natural gas had an influence on the performance of the combustion devices where the gas was used.
The exact measurement and standardization of the calorific value of NG are major factors of effective energy consumption and the process of estimating fuel quality. Several models of bomb calorimeter were utilized to measure the calorific value, specific heat, heat of reaction and latent heat of fuel[1-3].
The calorific value of gas was defined in ISO 6976 [4] as “the amount of heat which would be released by the complete combustion in air of a specific quantity of gas, in such a way the

Table 1. NG composition with geographic variations[5]

Source	Methane	Ethane	Propane	Butane	Nitrogen
Alaska	99.72	0.06	0.0005	0.0005	0.20
Algeria	86.98	9.35	2.33	0.63	0.71
Baltimore Gas & Electric	93.32	4.65	0.84	0.18	1.01
New York City	98.00	1.40	0.40	0.10	0.10
San Diego Gas & Electric	92.00	6.00	1.00	-	1.00

pressure p_1 at which the reaction takes place remains constant, and all of these products being in the gaseous state except for water formed by combustion, which is condensed to the liquid state at t_1." These specifications imply that the gas calorimeter should be designed so as to satisfy the definition.

Gas fuel has relatively low energy density compared with solid and liquid fuels, so a greater volume of gas fuel must be burned to measure its calorific value. For development of the gas calorimeter, the electric substitution method was applied for measuring the methane calorific value; this method was initiated by Alexandrov in IMM, Russia[6]. The calorimeter was designed such that Peltier elements gave off the heat supplied by the heater and the flame. During the steady state heat flow, we could measure the calorific value which substituted for the electric power. Freon-11 was applied as a heat carrier to keep the system in steady state heat flow.

It was proved that the measured calorific value of methane deviated - 0.36 % from the theoretical value. The design technique and the experimental data used here will be applied to establish the national standard for gas calorific value.

2. Operational Principle

The gas calorimeter was designed as a combustion chamber, a heat exchanging device, an insulator and a fuel and gas supply device, as shown in Fig. 1. Fuel with primary oxygen, secondary oxygen and argon were supplied to the combustion chamber. The compensation heater installed around the combustion chamber and the heat exchange pipe (copper) was welded at the upper part of the combustion chamber, through which the exhaust gas flows down to the bottom of the combustion chamber. When the gas was leaving the chamber, the thermal equilibrium state between the gas and the working fluid(Freon-11) was maintained.

The heat generated by the flame and the heater was transferred to the working fluid. The evaporated working fluid rose to Peltier elements and condensed at cooling fins. More specifically, the heat was transferred to the Peltier elements via the working fluid, and then the heat was pumped by the Peltier elements and flowed out with the cooling water of the Peltier elements.

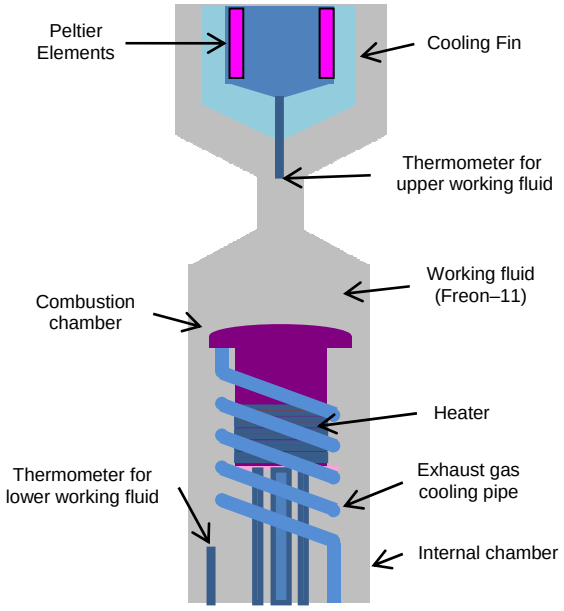

Fig. 1 Schematic of the flame calorimeter

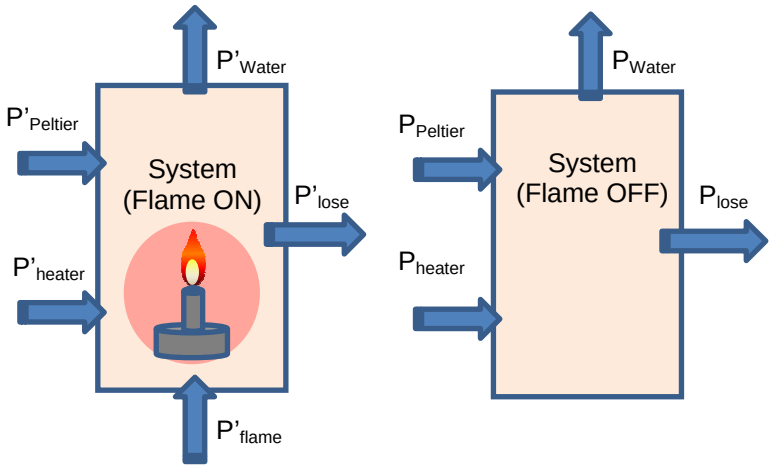

(a) Case A (b) Case B

Fig. 2 Schematic of energy balance.

Fig. 2 shows the energy balance during measurement in the system. The thermal equilibrium state was kept between the input and the output power (case A). The input power of P_{heater} and $P_{Peltier}$ were equal to the output power of the P_{water} and P_{lose}, and the equilibrium state was controlled according to the temperature of the lower working fluid which was kept constant under the equilibrium state. The power levels of P_{heater} and $P_{Peltier}$ were recorded. When the supply of the fuel gas (CH_4) was stopped (case B), then the equilibrium state was broken. With the increased power of P_{heater}, the equilibrium state could be achieved again. The difference of the P_{heater} between case A and case B was the power supplied by the flame. That is, the power supplied by the flame was substituted for the increased power of the P_{heater}.
The energy balances of the two cases were as follows:

$$\text{With flame (case A)} \quad P_w' + P_l' = P_h' + P_P' + P_f' \tag{1}$$

$$\text{Without flame (case B)} \quad P_w + P_l = P_h + P_P, \tag{2}$$

where the subscript w is the cooling water, P is Peltier elements, l is the losing power and f is the flame. From the above equations, the power of the fuel combustion was derived as:

$$P_f' = (P_w' - P_w) - (P_h' - P_h) - (P_P' - P_P) + (P_l' - P_l). \tag{3}$$

The calorific value of the fuel was measured without the uniform distribution of temperature in the calorimeter. Use of this method lessened the insulation difficulties in the calorimeter.

3. Design

The calorimeter system was designed as the combustion chamber, the cooling device, the insulation, the mass flowmeter for the fuel and the oxygen supply and the electric power supplier. Fig. 3 shows the mushroom shaped combustion chamber, the heater, the heater exchange pipe and the fuel supply device. During the burn, gas flows down through the spiral copper pipe, and the heat generated by the flame is transferred to the working fluid. The head and the column were made of stainless pipe, and their diameters were 105 mm and 61 mm, respectively. The fuel and the primary oxygen were supplied with 1.58 mm pipe and the secondary oxygen flow into the combustion chamber was supplied through coaxially installed 6.35 mm pipe. The igniter was

Fig. 3 Combustion chamber

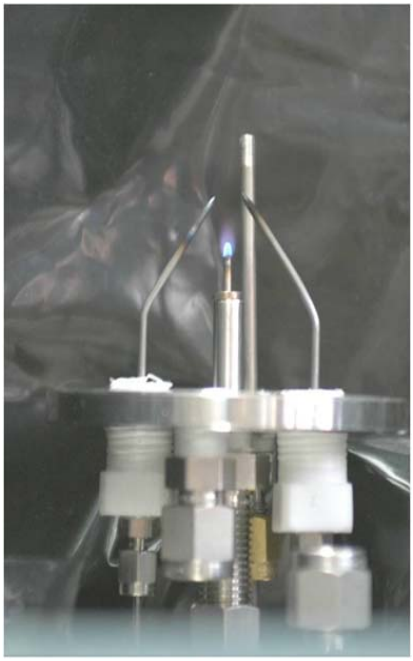

Fig. 4 Interior of the combustion chamber

Fig. 5 Internal chamber

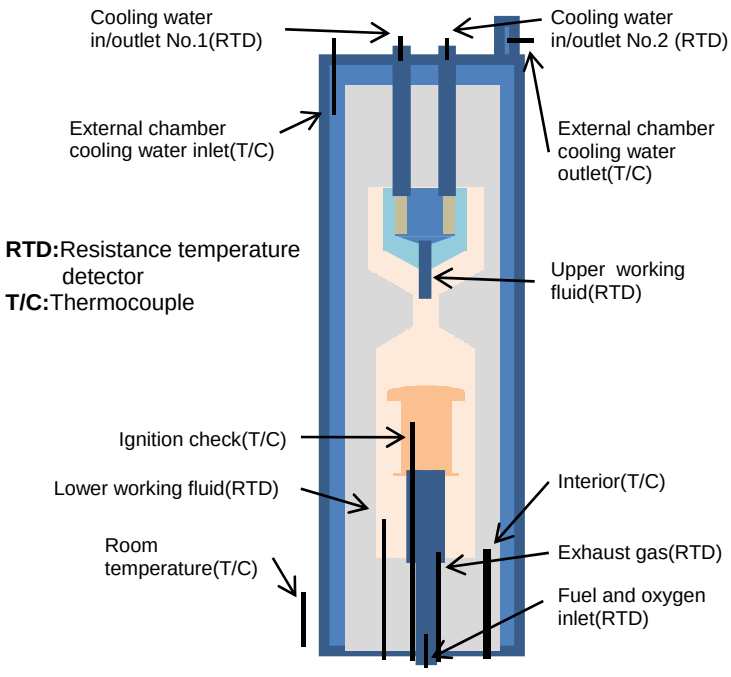

Fig. 6 Location of the temperature measuring points

connected from the bottom of the chamber and the line was insulated with ceramic bead.
For monitoring of the flame, the thermocouple was inside the chamber as shown in Fig. 4. The heater was made of nichrome wire 0.6 mm in diameter, 1.6 m in length and with a capacity of about 10 Ω . The heater was covered with a coating material for high temperature protection. The combustion chamber and the heater were installed in a dumbbell shaped internal chamber, shown

in Fig. 5. A volume of 1800 cc of the working fluid filled up the internal chamber just below the hat of the combustion chamber.
Then, the working fluid was vaporized by the heat from the flame and the heater and the gas went up to the cooling fin, which was at the top of the internal chamber. The two Peltier elements, which each had a capacity of 15 A of current, 15 V of voltage and a max. power of 110 W, were fixed to the outside of the cooling fin for heat pumping. The other side of the Peltier elements were cooled with 25 ℃ water. Eventually, the heat generated by the flame and the heater flowed into the working fluid via the Peltier elements and flowed out with the cooling water. Heat loss was the major source of uncertainty during the test. The internal chamber was set up within the external chamber. Between the two chambers, ceramic fiber was used for insulation. Water maintained at 25 ℃ flowed inside the external chamber for effective insulation.
Because the experiment was carried out under a steady state heat flow, the amount of heat inflow and outflow were measured with the fuel, the oxygen, the coolant and the exhaust gas. Fig. 6 shows the thermometers installed for the heat loss calculation and system control. The temperatures of the lower working fluid and the exhaust gas were reference values for whether the heat flow was steady state. The temperature of the lower working fluid, which was measured by RTD (Resistance Temperature Detector)sensor, was used for the control of the Peltier element input power. The temperature of the cooling water of the Peltier element and the external chamber were also measured for the calculation of heat flow. The temperature of the external chamber and the room temperature were applied to the heat loss calculation.
The flowrate of the fuel was directly related to the calorific value. The temperature of the cooling water for the Peltier element was also very sensitive to the calorific value. Thus, these were carefully controlled and stabilized, and the measured values are shown in Table 2. For exact measurement and effective insulation, the temperature of inflow and outflow reactants and the cooling water were maintained at 25 ℃ as much as possible.

Table 2. Average and standard deviation of flowrates of supplied reactants and water

	Case A						Case B	
	Ar	CH_4	Pri. O_2	Sec. O_2	Water1	Water2	Water1	Water 2
Average	40.18	40.36	26.28	156.64	425.97	299.85	423.90	301.17
Stand. Dev.	0.38	0.36	0.14	4.82	0.74	0.44	0.60	0.75

(Units: cc/min for chemical species, g/min for water)

4. Results and Discussion

Experiments were carried out with a flame (case A) and without a flame (case B). The test in case A measured the heater power under the stabilized conditions of the exhaust gas temperature at 25 ℃ and a fixed Peltier power. When the exhaust gas temperature was continued for 30 minutes at 25 ℃, the heat flow was estimated at a steady state. In the case B test, the heater power was measured under the fixed Peltier power of the case A test. When the difference of the lower working fluid temperature between the case A and B tests was less than 0.03 ℃ and continued more than 15 minutes, then we estimated that the heat flow was stabilized. Thus, the difference of the heater powers the case A and B tests was the calorific value of the fuel for the ideal case.
Fig. 7 shows the temperature of the exhaust gas and the lower working fluid under the steady state heat flow of the case A test. The power of the Peltier elements was fixed as 55.912W.

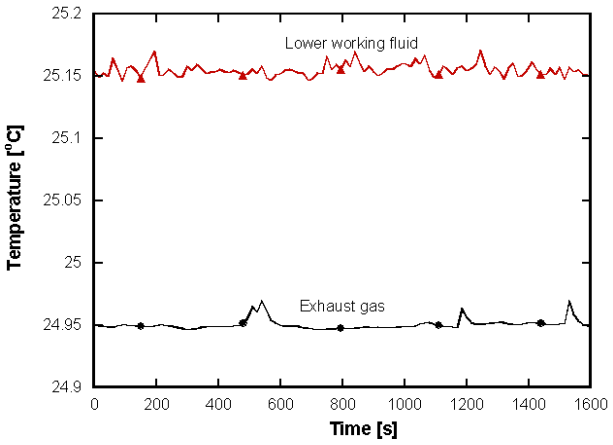

Fig. 7 The temperature of the lower working fluid and the exhaust gas as a function of time(Case A)

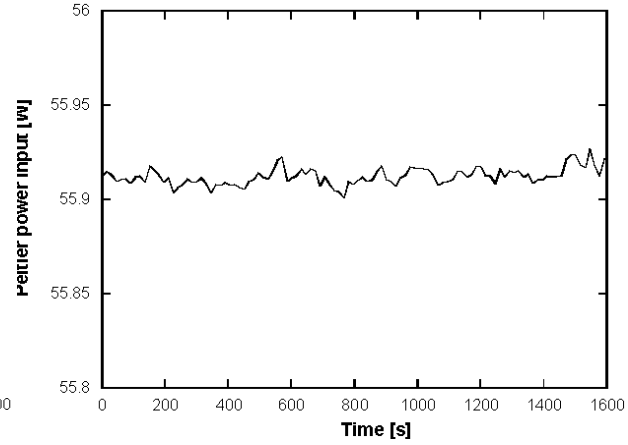

Fig. 8 Variation of the power supply to the Peltier element (Case A)

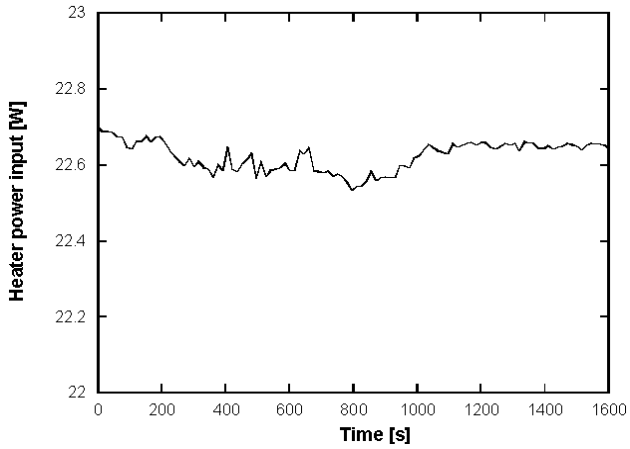

Fig.9 Variation of the power supply to the electric heater(Case A)

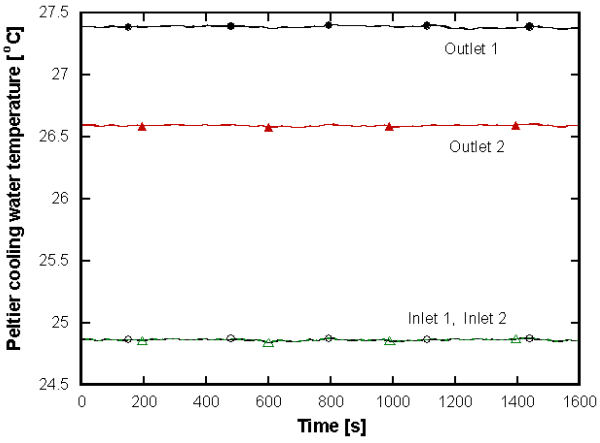

Fig. 10 Variation of Peltier cooling water temperature (Case A)

The exhaust gas temperature was stabilized at 24.945 ℃ for 1600 s, but some fluctuations were observed. These were due to the water drop on the temperature sensor. The average temperature of the lower working fluid will be used for the case B test as a reference value for system control. Figs. 8 and 9 show the power supplied to the Peltier elements and the heater. Fluctuations were relatively small, so we could conclude that the powers were stabilized. These meant that data in these figures were available for the calorific value calculation. The temperatures of the cooling water of the Peltier element were also stabilized, as shown in Fig. 10. The difference of the two outlet temperatures was due to the difference of flowrates.

For the case B test, the power of the Peltier elements was fixed as the same value as in the case A test and the heater power was controlled so as to keep the temperature of the lower working fluid at 25.154 ℃, as in the case A test. Fig. 11 shows the stabilization of the temperature variation of the working fluid for 2000 s; this stabilization indicates that the conditions of the case B test were sufficiently adjusted to those of the case A test. Figs. 12 and 13 show the power supply to the Peltier element and the heater. The Peltier element was fixed to reflect the value of the case A test.

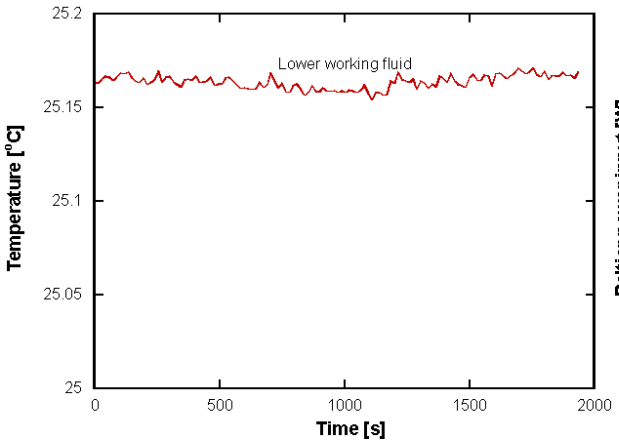

Fig. 11 Variation of the lower working fluid the temperature (Case B)

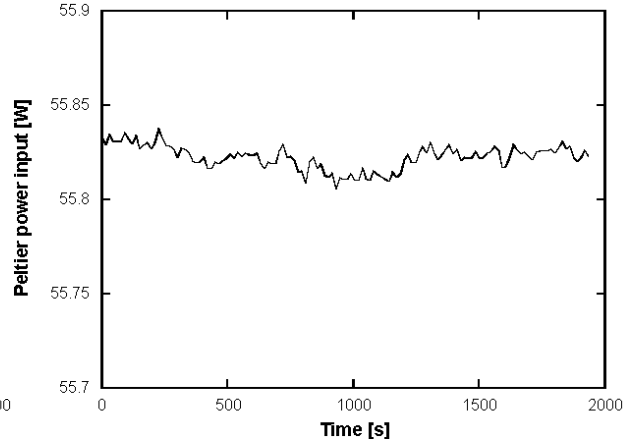

Fig. 12 Variation of the power supply to Peltier element (Case B)

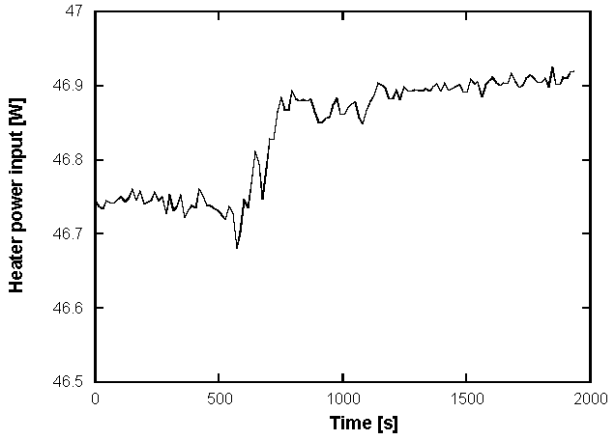

Fig. 13 Variation of the power supply to the electric heater (Case B)

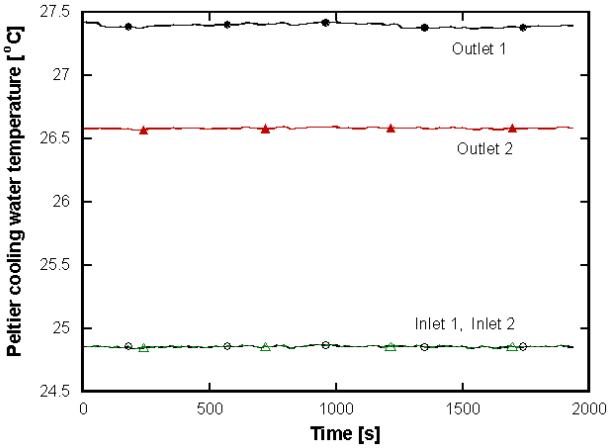

Fig. 14 Variation of Peltier cooling water temperature (Case B)

The heater power increased at 800 s, as shown in Fig. 13, which resulted from the power control program. A final value was available for the caloric value calculation. The temperature of the cooling water for the Peltier elements also kept constant, as shown in Fig. 14

Table 3 shows the measured temperatures and the powers under the stabilized heat flow. We know that the temperatures of the lower working fluid as the reference values coincided within ± 0.01 ℃ in both tests. However, the temperature of the external case and the cooling water of the Peltier elements, which should be kept at the same value, show some small differences. These differences indicate that heat loss occurred during the test. For the exact calculation of calorific value, these heat losses should be considered.

Heat loss could be considered as the conduction heat transfer through the side, the top and the bottom surface of the internal chamber. At the side surface, the heat transfers from the working fluid in the internal chamber to the external chamber through the internal chamber body, the insulation material, the acrylic tube and the air layer. The heat transfer at the side surface expressed as:[7]

Table 3. Average and standard deviation of the temperatures and the power inputs

Case		$T_{exhaust}$ (℃)	$T_{L.W.F.}$ (℃)	$T_{U.W.F.}$ (℃)	$T_{w1,in}$ (℃)	$T_{w1,out}$ (℃)	$T_{w2,in}$ (℃)	$T_{w2,out}$ (℃)
A	Average	24.945	25.154	23.941	24.862	27.386	24.862	26.589
	Stand. Dev.	0.0042	0.0051	0.0158	0.0067	0.0086	0.0067	0.0062
B	Average	24.903	25.164	23.909	24.856	27.394	24.856	26.582
	Stand. Dev.	0.0028	0.0038	0.0437	0.0060	0.0148	0.0060	0.0052

Case		$T_{Ext.\ chamber}$ (℃)	T_{O2} (℃)	T_{room} (℃)	Heater power (W)	Peltier power (W)
A	Average	24.177	24.261	21.537	22.565	55.912
	Stand. Dev.	0.0083	0.0257	0.0363	0.4371	0.0048
B	Average	25.366	24.578	21.355	46.892	55.822
	Stand.Dev.	0.0067	0.0063	0.0313	0.0672	0.0057

(where, L.W.F: lower working fluid, U.W.F.: upper working fluid)

$$Q = \frac{L(T_i - T_e)}{\frac{\ln(r_2 - r_1)}{2\pi k_1} + \frac{\ln(r_3 - r_2)}{2\pi k_2} + \frac{\ln(r_4 - r_3)}{2\pi k_3} + \frac{\ln(r_5 - r_4)}{2\pi k_4}}, \quad (4)$$

where L is length of the internal chamber, T_i is the working fluid temperature, T_e is room temperature, and k_1, k_2, k_3 and k_4 are the thermal conductivities of the stainless steel, the ceramic fiber, the acrylic and the air, which are 13.4 w/m/k, 0.12 w/m/k, 0.19 w/m/k and 0.02551 w/m/k, respectively. r_1 and r_2 are the inner and the outer diameters of the internal chamber, which are 0.068 m and 0.007 m, respectively. r_3 and r_4 are the inner and the outer diameters of the acrylic tube, which are 0.09 m and 0.01 m, respectively. r_5 is the inner diameter of external chamber, which is 0.11 m.

Calculation of heat loss was considered in two parts. The upper and the lower parts of the internal chamber were divided into the cooling and the heating regions, in which the reference temperatures were the upper and lower working fluid temperature, respectively.

Table 4. Heat loss through the side surface of the internal chamber

	Case A	Case B
Heat loss from upper part (W)	-0.029	-0.179
Heat loss from lower part (W)	0.220	-0.046
Total heat loss (W)	0.191	-0.225

The lengths of the upper and the lower parts were 0.265 m and 0.125 m, respectively. Finally, we derived the heat loss values shown in Table 4.
On the other hand, the heat lost at the top and the bottom surfaces moved from the stainless steel plate of the internal chamber to the stainless steel plate of the external chamber through the insulation material as expressed in Eq. (5)

$$Q = \frac{A(T_i - T_e)}{\frac{L_6}{k_1} - \frac{L_7}{k_2}}, \quad (5)$$

where T_i and T_e are the internal and external temperatures, respectively, k_1 and k_2 are the thermal conductivities of the stainless steel and the ceramic fiber, which are 13.4 w/m/k and 0.12 w/m/k, respectively. L_6 and L_7 are 0.005 m and 0.15 m, respectively. Heat loss is derived in Table 5.

Table 5. Heat loss through the upper and the lower plates of the internal chamber

	Case A	Case B
Heat loss from upper plate (W)	-0.004	-0.023
Heat loss from lower plate (W)	0.013	-0.003
Total heat loss(W)	0.009	-0.026

Finally, we derive the heat loss values of 0.200 W in case A and – 0.251 W in case B from Tables 4 and 5. We then know that the last term of Eq. (3) was $P_l' - P_l = 0.451$ W. With the experimental data in Table 3 and Eq. (3), the calorific value of the methane could be calculated as 24.475 W.
In order to estimate the accuracy of the measured caloric value of the methane, we compared the measured calorific value with the theoretical enthalpy of the chemical reaction. With the amount of the supplied methane, oxygen and argon in Table 2, the chemical reaction is expressed as:

$$CH_4 + 4.529O_2 + 0.995Ar \rightarrow CO_2 + 2H_2O + 2.529O2 + 0.995Ar. \quad (6)$$

We calculated the absolute enthalpy of the methane using STANJAN code[8] and the results are shown in Table 6.

Table 6. Absolute enthalpy of the mixtures evaluated using STANJAN code

	Water vapor mole fraction in the product	Liquid water mole fraction in the product	Absolute enthalpy kJ/(kg CH_4)
Reactants @21.54℃			-4707.9
Reactants @25℃			-4666.0
Products @25℃	0.000	0.307	-60161.9
Products @25℃	0.022	0.284	-59762.8
Products @24.95℃	0.000	0.307	-60160.6
Products @24.95℃	0.023	0.284	-59757.8

From Eq. (3), we have calculated the flame power (P_f') as 24.475 W. The flowrate of the methane supplied in this test was 4.462×10^{-7} kg/s, from Table 2. The calorific value of 1 kg methane was 24.275 w/(4.462×10^{-7} kg/s) = 54.852 MJ/kg. The reaction heat of the methane that is defined as the product should be the water at 25℃ only when 1 kg of methane is supplied at 25 ℃. From Table 6, we know that the reaction heat was -4666.0 – (- 60161.9) = 55.496 MJ/kg.
However, in this test, the methane was supplied at 21.54℃ instead of 25 ℃ and the products included the water vapor. Thus, the reaction heat was calculated as - 4707.9 - (- 59757.8)= 55. 050 MJ/kg. The measured calorific value of the methane underestimated the theoretical enthalpy by 0.36 %. The calorimeter measures the heat generated by the fuel. Therefore, the insulation was strongly related to accuracy. Deviation from the theoretical enthalpy implied that the heat loss should be more accurate. Heat loss was considered at the surface of the internal chamber, but the heat transfer through the electric wires and the fuel and the oxygen supplying pipes was not clearly described. Another reason for the deviation from theoretical enthalpy was the instability of the thermal equilibrium, which also came from the system insulation. Increased insulation and an elaborate heat transfer model for the calculation of heat loss would be helpful for increasing the accuracy of the calorimeter.

5. Conclusions

A gas calorimeter has been designed and characterized in this study. The calorimeter adopted the electric power substitution method based on Alexendrov's model. We measured the calorific value of methane and compared it with that of the theoretical enthalpy of the chemical reaction. The measured calorific value deviated - 0.36 % from the theoretical value. The deviation resulted from heat loss during the test, indicating that reinforced insulation for the system would increase the accuracy. The design technique and the experimental data from this study will be used for establishing the national standard for gas calorific value.

References

[1] The Japan Chem. Soc., Temperature • Heat, Pressure(Vol. 6 Chemical Thermo-dynamics and High-Pressure Science), The 5th Series of Experimental Chemistry, 2003.(in Japanese)
[2] P. Ulbig, D. Hoburg, 2003, Determinaton of the calorific value of natural gas by different methods, Thermochimica Acta, 2002, Vol. 382:27-35.
[3] L. I. Vorob'yov, T. G. Grishchenko, and L. V. Dekusha, Review : bomb calorimeters for determination of the specific combustion heat of fuel, Journal of Engineering Physics and Thermophysics, 1997,Vol 70, No.5.
[4] ISO 6976, Natural gas-Calculation of calorific values, density, relative density and Wobbe index from composition, 2002.
[5] Liquid methane fuel characterization and safety assessment report, Cryogenic Fuels. Inc., Report No. CFI-1600, Dec. 1991.
[6] Yuri I. Alexandrov, Estimation of the uncertainty for an isothermal precision gas calorimeters, Thermochimica Acta, 2002, Vol. 382.:55-64.
[7] Yunus A. Cengel, "Heat transfer," 2ed, 2004, McGraw-Hill Korea.
[8] Reynolds, W. C., STANJAN-Interactive computer programs for chemical equilibrium analysis, Department of Mechanical Engineering, Stanford University, 1995.